JTTEE 3:51-56

Indentation Method for Fracture Resistance Determination of Metal/Ceramic Interfaces in Thick TBCs

R. Dal Maschio, V.M. Sglavo, L. Mattivi, L. Bertamini, and S. Sturlese

The indentation technique has been used to measure the adhesion of plasma-sprayed ceramic coatings on metals intended for thick thermal barrier coating (TTBC) applications. This approach provides the adhesion value as the critical strain energy release rate, G_c, of the interface, which also takes into account any residual stresses. The theoretical background of the method is outlined, and specific examples are reported with respect to the effect of substrate temperature on the metal/ceramic adhesion of thick TBCs.

1. Introduction and State-of-the-Art

A WIDE range of tests have been developed to measure the adhesion of thermal spray coatings.[1,2] Although these tests can be useful for ranking purposes, many of them do not measure a unique adhesion parameter, and comparison among the different tests can be difficult. Furthermore, several of these tests are sensitive to the presence of flaws, because the initiation of failure represents the critical stage.

More rigorous interfacial toughness tests, based on the linear elastic fracture mechanics of bimaterial interfaces, have been proposed. These can be broadly divided for application to planar interfaces into sandwich geometries and delamination tests.

The common feature of the specimens in the former test is that each of them is homogeneous, except for a very thin layer of different material that is sandwiched between the two halves, which comprises the bulk of the specimen. The thickness of the layer is typically a hundredth or even a thousandth of the length scale of the overall geometry, with a pre-existing crack lying along one of the interfaces. They include double cantilever beam,[3,4] single-edge notch,[5,6] compact tension,[6] double torsion,[6] cracked Brazilian disk (Brazilian nut),[7] and four-point shear.[8] Although the last two test geometries have not been reported widely in the plasma spray field, in all of the other tests, critical strain energy release rate, G_c, or toughness, K_{Ic}, has been evaluated by means of formulations determined for homogeneous specimens with no layer to characterize the interface crack in the presence of the layer. Nevertheless, with all of these geometries, it will be possible to cover a range of proportions of opening (Mode I) to shear (Mode II) loading at the crack tip, a factor which affects the measured G_c.[9]

Keywords: adhesion, fracture toughness, indentation methods, interface properties, substrate temperature, thermal barrier coatings, yttria-stabilized zirconia, ttbcs, vickers indentation

R. Dal Maschio, V.M. Sglavo, and L. Mattivi, Universita Degli Studi Di Trento, Dipartimento di Ingegneria Dei Materiali, Via Mesiano, 77, 38050 Trento, Italy; **L. Bertamini,** C.S.M. Cire di Pergine, Trento, Italy; and **S. Sturlese,** C.S.M. S.p.A., P.O. 10747, Roma Eur, Italy.

Charalambides et al.[11,12] have developed a four-point bend test that has been applied to plasma spray specimens. Howard and Clyne[10] accounted for the residual stress contribution to the G_c value proposed by Charalambides et al.[12] by inserting a residual stress profile predicted by a numerical model.[13] Their results, which used a material system of titanium on titanium alloy (Ti-6Al-4V), showed an underestimation of G_c without considering residual stresses, which is not of general application in the field of TTBCs. For example, consider a typical TTBC system of a ZrO_2-8wt% Y_2O_3 ceramic coating (about 1.5 mm thick) sprayed at temperatures of about 100 to 150 °C (to achieve low residual compression stresses) on a NiCoCrAlY coat (about 300 μm thick) on a superalloy substrate. According to the calculations performed by Charalambides et al,[12] it is possible to foresee that the G_c value for this TTBC system in a four-point bend test is influenced by the residual stress field. Thus, all these fracture mechanics techniques are fairly complex and are not easily available for quality control.

The aim of this article is to describe a procedure based on the indentation technique that allows G_c of metal/ceramic interfaces to be evaluated in a reliable and simple fashion. This parameter will be used to characterize the fracture resistance of the interface as a function of the substrate temperature in TTBCs. The consistency of the results will be confirmed by thermal fatigue tests.

2. *Theoretical Concepts*

The metal/ceramic interface was characterized by making Vickers indentations on the interface between the bonding layer and ceramic coating (Fig. 1). In this manner, median cracks, starting from the indentation site corners, propagate along the interface with a substantial semicircular front. A "hemispherical" plastic zone is formed under the indentation site, and the mismatch between elastic and plastic deformations on the unloading part of the indentation cycle causes a net outward force acting on the crack. The experimental situation can be well represented in a two-dimensional manner, as shown in Fig. 2 where an interfacial crack of length $2c$ is partially loaded by a constant pressure $t(x)$. From a theoretical point of view, this situation is intermediate between that of an interfacial crack loaded perpendicularly by a concentrated force (P in Fig. 3) and that of an in-

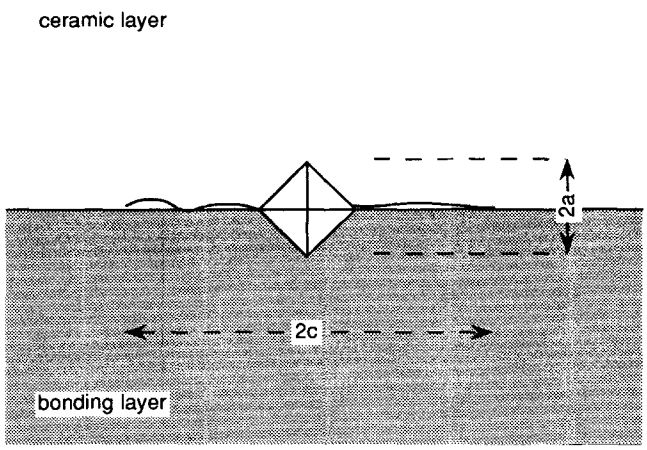

Fig. 1 Schematic of an interfacial Vickers indentation

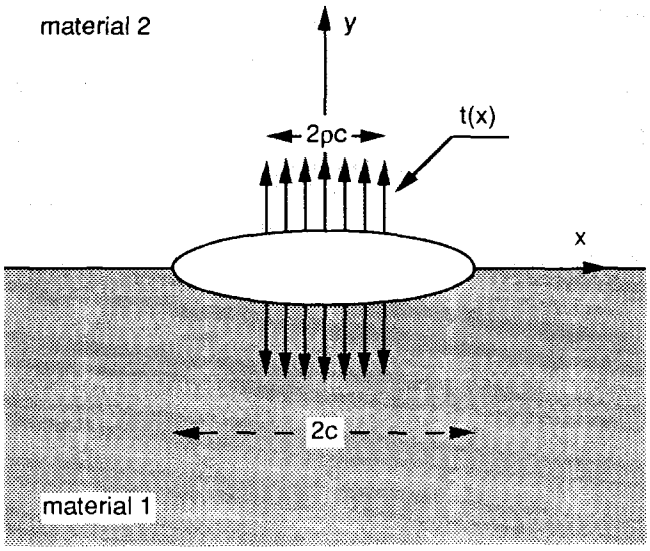

Fig. 2 Two-dimensional representation of an interfacial crack with $2c$ length partially loaded ($2\rho c$) by a constant pressure t

terfacial crack uniformly loaded by a constant pressure $t(x)$ (Fig. 4). According to Rice and Sih,[14] G for conditions as shown in Fig. 3 is

$$G = \frac{1}{\pi^2}(C_1 + C_2) P^2 \sin^2(\varepsilon \log(2c)) \frac{1}{c} \qquad [1]$$

where

$$C_i = \frac{k_i + 1}{G_i} \text{ and } i = 1,2$$

$$k_i = \begin{cases} 3 - 4\nu_i \text{ (plane strain)} \\ \dfrac{3 - \nu_i}{1 + \nu_i} \text{ (plane stress)} \end{cases} \qquad i = 1,2$$

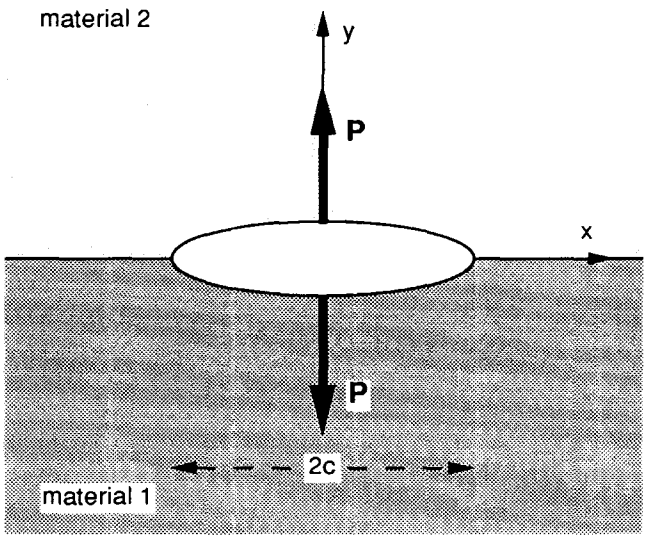

Fig. 3 Two-dimensional representation of an interfacial crack perpendicularly loaded by a concentrated force P

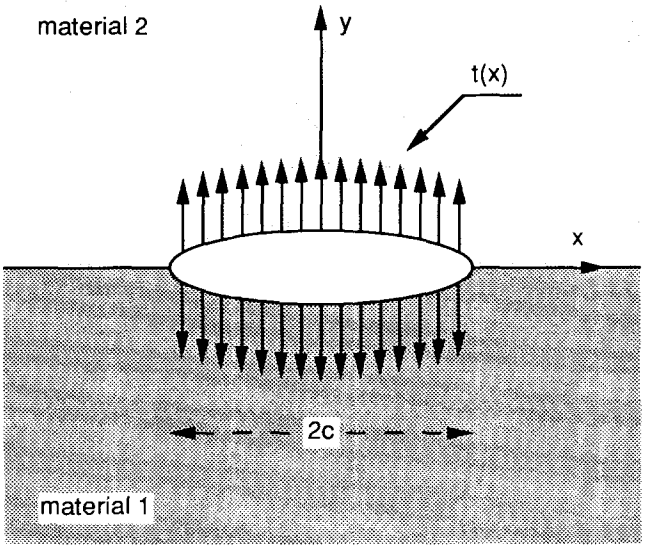

Fig. 4 Two-dimensional representation of an interfacial crack uniformly loaded by a constant pressure t

$$\varepsilon = \frac{1}{2\pi} \log \left(\frac{\dfrac{k_1}{G_1} + \dfrac{1}{G_2}}{\dfrac{k_2}{G_2} + \dfrac{1}{G_1}} \right)$$

and G_i are the shear elastic moduli; ν_i is the Poisson's ratio; $2c$ is the interfacial crack length; and P is the concentrated force. The subscripts 1 and 2 refer to the two different materials.

For the conditions shown in Fig. 4, Willis[15] calculated G with the following expression:

$$G = \frac{\pi^2}{2}\frac{(b^2 - d^2)}{b}(1 + 4k^2)t^2c \quad [2]$$

where

$$b = \frac{(1-\nu_1)}{2\pi G_1} + \frac{(1-\nu_2)}{2\pi G_2}$$

$$d = \frac{(1-2\nu_1)}{4\pi G_1} - \frac{(1-2\nu_2)}{4\pi G_2}$$

$$k = \frac{1}{2\pi}\ln\left(\frac{b+d}{b-d}\right)$$

Equation 1 can be rewritten as:

$$G = A\frac{P^2}{c} \quad [3]$$

where A is a constant depending on material properties. Equation 2 can be rewritten as:

$$G = A' t^2 c \quad [4]$$

where A' is a constant that is related to material properties. Equation 4 is similar to Eq 3, bearing in mind that the result of the distributed pressure $t(x)$ is $2 \cdot t(x) \cdot c$.

The similarity between Eq 3 from Rice and Sih and Eq 4 from Willis supports the authors' choice to follow the approach of Willis, which better simulates the current experimental conditions as represented in Fig. 2. The parameter G is now expressed by:

$$G = A'' t^2 c \quad [5]$$

where the constant A'' includes another constant ρ, which is related to the nonuniform distribution of pressure t on the entire crack length.

The next step involves evaluating the pressure t in terms of experimental quantities related to interfacial indentation. According to Johnson,[16] the plastic zone in any homogeneous material exhibits a substantially hemispherical shape whose dimensions are affected by the elastoplastic properties of the material. The plastic zone radius b is given by:

$$\left(\frac{b}{a}\right)^3 = \frac{\frac{E\tan\beta}{\sigma_y} + 4(1-2\nu)}{6(1-2\nu)} \quad [6]$$

where a is the indentation semidiagonal; E is the Young modulus, σ_y is the yield stress, and $\beta = 19.7°$ for a Vickers indenter.

Equation 6 is valid only for homogeneous materials, but can be extended to a bimaterial interface indentation if the appropriate median values for the elastoplastic properties of both materials are considered. Assuming that there is no interference between the two materials, one can define the average radius, b_{av}, of the plastic zone as:

$$b_{av} = \frac{b_1 + b_2}{2} \quad [7]$$

where b_i ($i = 1,2$) are the plastic zone radii corresponding to the sandwiched materials.

The hypothesis of no interference between the two materials has been verified by a simplified finite-element model (FEM), using ABAQUS code.[17] Bousinnesq solutions for the problem of a concentrated force acting on a monomaterial and on a bimaterial interface are shown in Fig. 5(a) and (b), respectively. The contours in Fig. 5 represent stress levels across the thickness (i.e., in cross section) of the material system. In the second case, the contours corresponding to the same level of stress equivalent σ_{eq}, defined according to Von Mises criterion,[18] show a narrow link zone between the two half plastic zones, thus corroborating the hypothesis of no interference. The Bousinnesq approach does not represent a real indentation; however, because it is a simple model, it has use in characterizing the behavior of a bimaterial interface.

The plastic zone is a source of an outward residual force acting on the crack, and this force arises from the mismatch between elastic and plastic deformations. Therefore, the boundary of the plastic zone is subjected to a stress field corresponding to

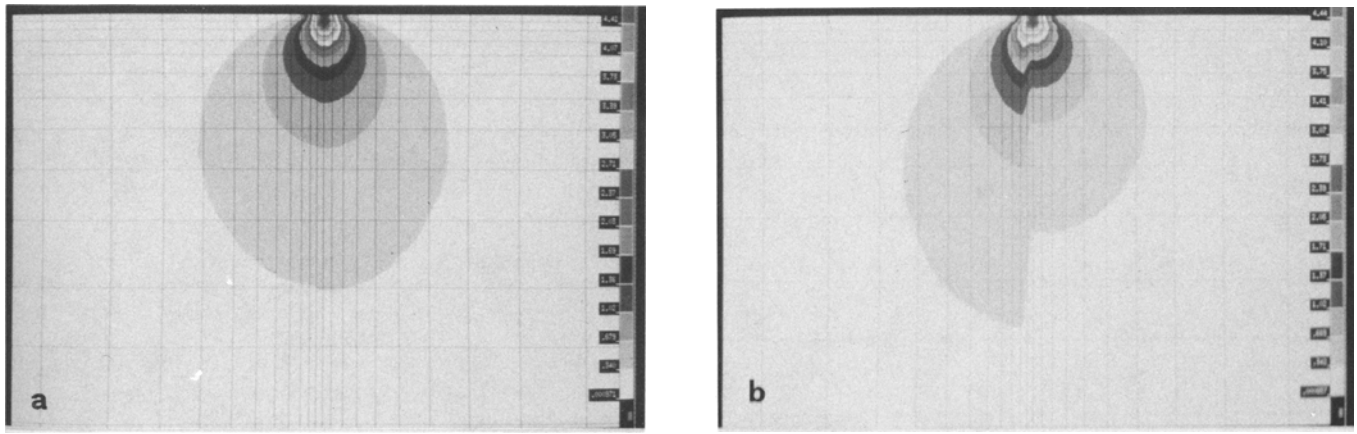

Fig. 5 FEM analysis of a Bousinnesq problem. (a) Monomaterial. (b) Bimaterial interface. The contours represent equivalent stress, σ_{eq}, levels according to an arbitrary scale based on colors (right) across the thickness of the material system

the deformations developed if the plastic zone was released from the surrounding material.

According to arguments by Lawn et al.[19] in the hypothesis of representing these stresses by a constant hydrostatic compression p on the plastic zone boundary, it is possible to write:

$$p = 2\frac{\delta V}{V}\frac{1}{\left(\frac{1}{E_1}+\frac{1}{E_2}\right)} \quad [8]$$

where V and δV are the volume of plastic zone and impression (or volume change), respectively.

The magnitude of the effective outward residual force on the crack can be obtained by integrating the horizontal stress component over the zone cross section within the crack plane. The net outward force, P_r, applied to the center of the interfacial crack is

$$P_r \propto p V^{2/3} \quad [9]$$

This situation is similar from a fracture mechanics point of view to that studied by Willis[15] and can be expressed as:

$$t \propto \frac{P_r}{c^2} \quad [10]$$

$G = G_c$ can be put on the unloading part of the indentation cycle when a median crack of extension πc, emanating from an indentation site corner along the interface has a driving force due only to the plastic zone hydrostatic stress. Thus,

Table 1 Powder Characteristics

Bond coat	Ceramic coating
HCST (Stark) L AlSil2(a)	Metco 204NS(b)
Al-12Siwt%	ZrO_2-8Y_2O_3wt%
−45 μm	−106 + 10 μm

(a) H.C. Starck GmbH & Co. KG, D-6000, Dusseldorf, Germany. (b) Metcó (Perkin-Elmer), Westbury, NY 11590 USA

Table 2 Spray Parameters

Power, kW	28
Stand-off gun distance, cm	11
Gas flow rate, L/min	40 Ar + 12 H_2
Powder flow rate, kg/h	1.5
Relative velocity of torch, mm/s	600

$$G_c = \alpha\left[\frac{b^2-d^2}{b}(1+4k^2)\right]\psi\frac{a^4}{c^3} \quad [11]$$

where b, d and k have the same expressions in Eq 2, and ψ is defined as:

$$\psi = \frac{1}{\left(\frac{1}{E_1}+\frac{1}{E_2}\right)^2}\frac{1}{\left(\sqrt{\frac{E_1}{H_1}}+\sqrt{\frac{E_2}{H_2}}\right)^2} \quad [12]$$

H is the hardness, and parameter α is a numerical constant that incorporates all numerical constants independent of the system indenter or specimen. The value of α can be deduced from Ref 19 if Material 1 is the same as Material 2, bearing in mind the equivalence between strain energy release rate, G, and stress intensity factor, K. Under these conditions, α equals 0.0197.

3. Experiments and Results

Aluminum specimens 40 × 50 × 5 mm were sprayed with a PS4180 SNMI Plasma Set using a TS6-type torch, mounted on a IRBL6 Asea Robot fastened to a rotating table. Details of the powders used are shown in Table 1. The aluminum substrates were grit blasted and ultrasonically cleaned before spraying. Spraying parameters used for the deposition of the bond and top layer coatings are summarized in Table 2.

Substrate temperature was kept constant during each spray run using a front air cooling system for air plasma spraying (APS) or liquid argon cooling system for atmosphere- and temperature-controlled spraying (ATCS). The substrate temperature was systematically varied for ceramic coatings only. The bonding coat was sprayed at a substrate temperature of 150 °C for all samples.

The deposition temperature was measured using a K-type thermocouple, inserted in a 4-mm depth hole in the back of the sample, linked to an *XY* Linseis recorder and stored by a PC system. The full set of samples used for this analysis is detailed in Table 3. A set of three samples was prepared for each spraying condition.

Beams 5 × 20 mm were cut using a diamond saw from coated plates and polished with SiC papers and diamond paste of 3 μm. Physical characterization included optical and electron microscopy and bulk density evaluation by Archimede's method (Table 4). Mechanical characterization was carried out by measuring the Vickers hardness and Young's modulus by the Knoop indentation method for both sprayed layers[20] (Table 5 and Fig. 6). These moduli values have been used to calculate the critical strain energy release rate, G.

Table 3 Substrate Temperature under Different Spraying Conditions for the Bond Coat and Ceramic Overlay

	Bonding layer		Ceramic coating	
Sample Code	Deposition temperature, °C	Thickness, mm	Deposition temperature, °C	Thickness, mm
APS1	150	1.70	120	2.00
APS2	150	1.50	230	2.10
APS3	150	1.60	350	2.10
ATCS	150	1.75	50	2.05

The effect of deposition temperature on the density, hardness, and Young's modulus of the ceramic coating for the APS samples is evident. An increase in the deposition temperature would be expected to densify the structure.

The adhesion between the metallic bond coat and the ceramic top layer, as measured by the critical strain energy release rate of the interface, was determined by making a set of Vickers indentations (using loads of 50 and 100 N), at the ceramic/bond interface according to the setup depicted in Fig. 1. Care was taken to align the indenter diagonal with the interface.

Cracks and indentation diagonals lengths were measured by optical and/or electron microscopy. Figure 7 shows a typical deformation and fracture pattern after the indentation test. By assuming typical Poisson's ratios of 0.25 and 0.30 for the ceramic layer and bond layer, respectively, G_c values can be calculated for the different samples (Table 6); these are the average values of about ten indentations for each load and for each sample.

Thermal fatigue tests were performed on 40 × 24 mm samples using a vertical furnace with an alumina tube. The cycle consisted of 12 min of heating at 600 ± 5 °C and 8 min of cooling in still air. Temperature was measured using a K-type thermocouple closed to the sample and connected to a recorder. Table 7 summarizes the thermal fatigue test results and indicates the number of cycles corresponding to the start of spallation and to complete spallation of the ceramic coating as determined by visual inspection.

4. Discussion

Toughness values measured for any bimaterial interface take into account two different contributions. The first is directly connected to the quality of the coupling of the two materials; the second is related to the residual stress field.

There are various effects of the substrate temperature. As the substrate temperature increases, there is an improvement in adhesion due to improved mechanical interlocking between ceramics and metallic layers because of higher wettability. If an air spray process is used, there is also increased oxidation of the metallic bond layer. Also, the residual stress field increases in the case of different thermal expansion coefficients.

The method proposed in this article for G_c measurement provides a trend of values substantially in agreement with these concepts. Under the experimental conditions of this work, the best compromise among these phenomena was obtained at a deposition temperature of about 230 °C (see Tables 3 and 6). Thermal fatigue test results show a reasonable correlation with

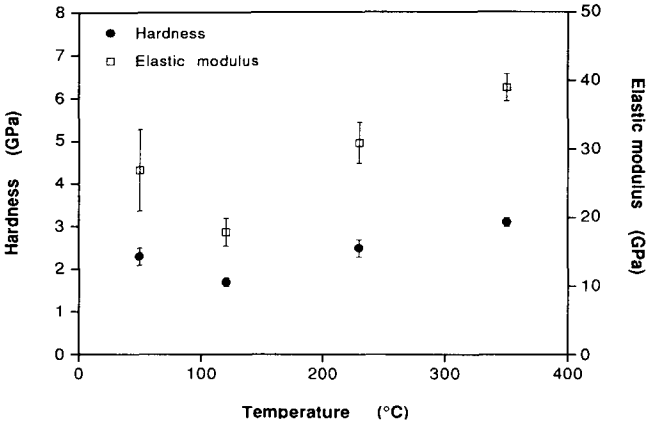

Fig. 6 Mechanical properties versus deposition temperature for ceramic coating

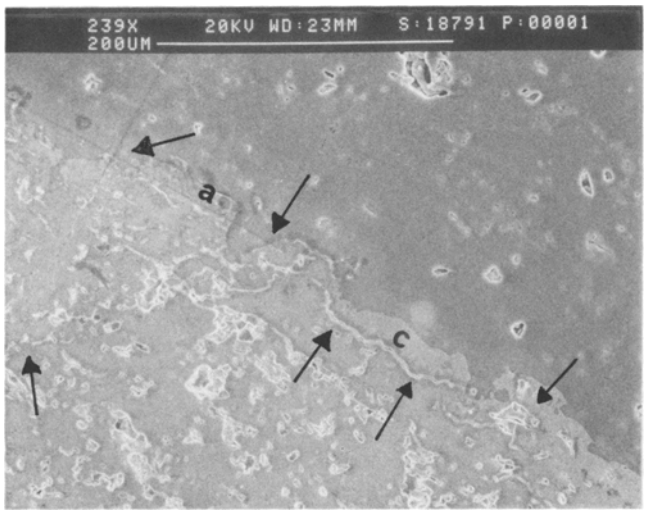

Fig. 7 SEM micrograph of the interface after indentation. Indentation site (a) and propagated crack (c) are observed

Table 4 Bulk Density (g/cm^3) of the Bond Coat and Ceramic Overlay

Sample code	Bonding layer	Ceramic layer
APS1	2.2 ± 0.2	4.9 ± 0.5
APS2	2.3 ± 0.2	5.1 ± 0.5
APS3	2.3 ± 0.2	5.3 ± 0.4
ATCS	2.7 ± 0.3	5.4 ± 0.5

Table 5 Hardness and Elastic Moduli of the Coating System

	Bonding layer		Ceramic coating	
Sample code	Hardness, GPa	Elastic modulus, GPa	Hardness, GPa	Elastic modulus, GPa
APS1	1.0 ± 0.1	18 ± 1	1.7 ± 0.1	18 ± 2
APS2	0.8 ± 0.1	26 ± 3	2.5 ± 0.2	31 ± 3
APS3	0.5 ± 0.1	9 ± 1	3.1 ± 0.1	39 ± 1
ATCS	1.0 ± 0.1	34 ± 5	2.3 ± 0.2	27 ± 6

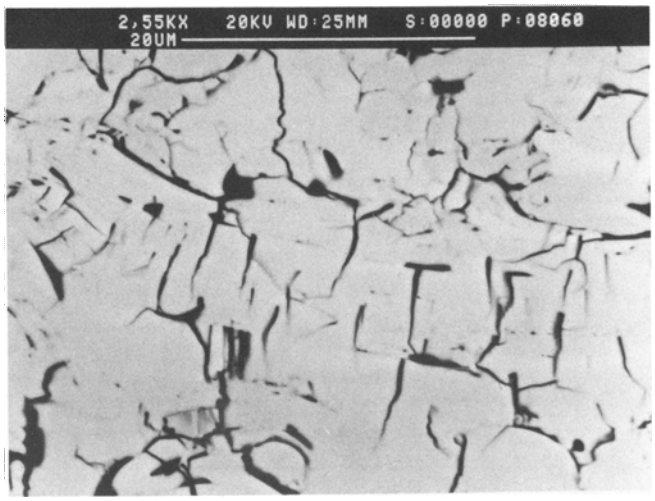

Fig. 8 SEM micrograph of ATCS ceramic coating cross section

Table 6 Critical Strain Energy Release Rate

Sample code	G_c, J/m^2, at: 50 N	100 N
APS1	11.1 ± 1.3	10.4 ± 1.3
APS2	16.0 ± 1.0	21.2 ± 1.2
APS3	5.7 ± 0.9	3.8 ± 0.5
ATCS	5.3 ± 0.5	5.8 ± 0.7

Table 7 Thermal Fatigue Test Results

Sample code	Spallation initiation	Total spallation
APS1	190	700
APS2	600	1150
APS3	100	600
ATCS	400	1100

the G_c values, at least for the APS samples. This arises due to bond coat oxidation and thus a residual stress field increase.

Different behavior is observed for the ATCS samples. A low critical strain energy release rate value corresponds to high thermal fatigue resistance. First of all, the metallic bond coating in ACTS samples is not oxidized, and the intensity of the residual stress field is low. The good performance of the ATCS samples in thermal fatigue tests is due to the combined effect of low residual stress field and an unoxidized interface. These features, connected to a diffuse microcracking pattern (Fig. 8), suggest that stresses developed during the thermal transient do not strongly influence the interface. Nevertheless, low G_c values are related to low wetting of the substrate during plasma spraying process.

5. Conclusion

A method for evaluating adhesion in TTBCs has been proposed. It is based on a fracture mechanics approach of the Vickers indentation technique and allows the interfacial critical energy release rate to be obtained. As an example of the application of this method, the dependence of adhesion on deposition temperature has been considered. The consistency of the results is confirmed by thermal fatigue tests of samples sprayed in air.

Future steps for improving the indentation test will be the evaluation of phase angle, to compare this methodology with the other fracture mechanics tests.[3,8] The influence of the residual stress field on G_c values will also be considered.

References

1. D.S. Rickerby, A Review of the Methods for the Measurement of Coating-Substrate Adhesion, *Surf. Coat. Technol.*, Vol 36, 1988, p 541-555
2. H. Gruntzner, A Comparison of Different Adhesion Test Methods for Thermally Sprayed Coatings, *Proc. 2nd Plasma Technik Symp.*, P. Huber and H. Eschnauer, Ed., Lucerne, 1991, p 351-357
3. P. Ostojic and R. Mc Pherson, Determining the Critical Strain Energy Release Rate of Plasma-Sprayed Coatings using a Double Cantilever Beam Technique, *J. Am. Ceram. Soc.*, Vol 17, 1988, p 891-899
4. G.N. Heintze and R. Mc Pherson, A Further Study of the Fracture Toughness of Plasma-Sprayed Zirconia Coatings, *Surf. Coat. Technol.*, Vol 36, 1988, p 125-132
5. T. Suga, I. Kvernes, and G. Elssner, *Z Werkstofftech.*, Vol 15, 1989, p 371-377
6. G. Kleer, R. Schonholz, W. Doll, S. Sturlese, and N. Zacchetti, Interface Crack Resistance of Zirconia Base Thermal Barrier Coatings, *High Performance Ceramic Films and Coatings*, P. Vincenzini, Ed., Elsevier, 1991, p 329-338
7. J.S. Wang and Z. Suo, Experimental Determination of Interfacial Fracture Toughness Curves Using Brazil-Nut-Sandwiches, *Acta Met. Mater.*, Vol 38, 1990, p 1279-1290
8. M.Y. He, Mixed Mode Fracture: The Four Point Shear Specimen, *Acta Metall.*, Vol 38, 1990, p 839-846
9. H.C. Cao and A.G. Evans, An Experimental Study of the Fracture Resistance of Bimaterial Interfaces, *Mech. Mater.*, Vol 7, 1989, p 295-304
10. S.J. Howard and T.W. Clyne, Interfacial Fracture Toughness of Vacuum-Plasma-Sprayed Coatings, *Surf. Coat. Technol.*, Vol 45, 1990, p 333-342
11. P.G. Charalambides, J. Lund, A.G. Evans, and R.M. Mc Meeking, A Test Specimen for Determining the Fracture Resistance of Bimaterial Interfaces, *J. Appl. Mech. (Trans. ASME)*, Vol 56, 1989, p 77-82
12. P.G. Charalambides, H.C. Cao, J. Lund, and A.G. Evans, Development of a Test Method for Measuring the Mixed Mode Fracture Resistance of Bi-Material Interfaces, *Mech. Mater.*, Vol 8, 1990, p 269-283
13. S.C. Gill and T.W. Clyne, Stress Distributions and Material Response in Thermal Spraying of Metallic and Ceramic Deposits, *Metall. Trans. B*, Vol 21, 1990, p 377-385
14. J.R. Rice and G.C. Sih, Plane Problems of Cracks in Dissimilar Media, *J. Appl. Mech.*, Vol 32, 1965, p 418-423
15. J.R. Willis, Fracture Mechanics of Interfacial Cracks, *J. Mech. Phys. Solids*, Vol 19, 1971, p 353-368
16. K.L. Johnson, *Contact Mechanics*, Cambridge University Press, 1985, p 175
17. *ABAQUS User's Manual*, Hibbit, Karlsson ans Sorenson, Providence, RI, 1990
18. J. Lemaitre and J.L. Chaboche, *Mécanique des Matériaux Solides*, Dunod, Paris, 1985, p 53
19. B.R. Lawn, A.G. Evans, and D.B. Marshall, Elastic/Plastic Indentation Damage in Ceramic: The Median/Radial Crack System, *J. Am. Ceram. Soc.*, Vol 63, 1980, p 574-581
20. D.B. Marshall, T. Noma, and A.G. Evans, A Simple Method for Determining Elastic Modulus to Hardness Ratio Using Knoop Indentation Measurement, *J. Am. Ceram. Soc.*, Vol 65, 1982, p 175-176